2012

# Modeling clear-sky solar radiation across a range of elevations in Hawai'i: Comparing the use of input parameters at different temporal resolutions

Ryan J. Longman
*University of Hawai'i at Mānoa*

Thomas W. Giambelluca
*University of Hawai'i at Mānoa*

Abby Frazier
afrazier@clarku.edu

# Modeling clear-sky solar radiation across a range of elevations in Hawai'i: Comparing the use of input parameters at different temporal resolutions

Ryan J. Longman,[1] Thomas W. Giambelluca,[1] and Abby G. Frazier[1]

Received 13 June 2011; revised 4 November 2011; accepted 11 November 2011; published 19 January 2012.

[1] Estimates of clear sky global solar irradiance using the parametric model SPCTRAL2 were tested against clear sky radiation observations at four sites in Hawai'i using daily, mean monthly, and 1 year mean model parameter settings. Atmospheric parameters in SPCTRAL2 and similar models are usually set at site-specific values and are not varied to represent the effects of fluctuating humidity, aerosol amount and type, or ozone concentration, because time-dependent atmospheric parameter estimates are not available at most sites of interest. In this study, we sought to determine the added value of using time dependent as opposed to fixed model input parameter settings. At the AERONET site, Mauna Loa Observatory (MLO) on the island of Hawai'i, where daily measurements of atmospheric optical properties and hourly solar radiation observations are available, use of daily rather than 1 year mean aerosol parameter values reduced mean bias error (MBE) from 18 to 10 W $m^{-2}$ and root mean square error from 25 to 17 W $m^{-2}$. At three stations in the HaleNet climate network, located at elevations of 960, 1640, and 2590 m on the island of Maui, where aerosol-related parameter settings were interpolated from observed values for AERONET sites at MLO (3397 m) and Lāna'i (20 m), and precipitable water was estimated using radiosonde-derived humidity profiles from nearby Hilo, the model performed best when using constant 1 year mean parameter values. At HaleNet Station 152, for example, MBE was 18, 10, and 8 W $m^{-2}$ for daily, monthly, and 1 year mean parameters, respectively.

**Citation:** Longman, R. J., T. W. Giambelluca, and A. G. Frazier (2012), Modeling clear-sky solar radiation across a range of elevations in Hawai'i: Comparing the use of input parameters at different temporal resolutions, *J. Geophys. Res.*, *117*, D02201, doi:10.1029/2011JD016388.

## 1. Introduction

[2] Accurate surface solar radiation observations are essential for studies of solar energy resource availability, ecosystem processes, hydrological processes, and climate change. Variations in solar radiation exert strong control on the terrestrial environment by regulating available energy at the surface for evapotranspiration and photosynthesis. Surface solar radiation observations are important for estimating these processes and for assessing air quality and cloud cover through their effects on temporal variation in solar intensity. When direct measurements are not available, models are often used to make predictions of solar radiation under clear sky conditions, which, combined with cloud cover estimates, can be used to simulate solar radiation under all conditions [*Alados-Arboledas et al.*, 2000; *Alados et al.*, 2002]. Clear sky solar radiation models can be tested by comparing predictions to observed measurements during cloud-free periods [*Gueymard*, 2003b].

[3] Two types of models are commonly used to estimate clear sky spectral irradiance at the Earth's surface. The first type utilizes a radiative transfer scheme which takes into account the vertical profiles of gaseous and aerosol constituents, represented as a series of scattering and absorption layers in the atmosphere [*Jacovides et al.*, 2004]. Examples of this type of model are the commonly used LOWTRAN 7 [*Kneizys et al.*, 1980] and a higher resolution model called MODTRAN [*Anderson et al.*, 1993]. These models are not applicable for all situations, due to long execution times and their extensive input parameter requirements [*Tadros et al.*, 2005]. The second, more simplified type of radiation model approximates atmospheric transmission through a single homogeneous layer of the atmosphere in which extraterrestrial radiation diminishes as a result of several absorption and scattering processes [*Leckner*, 1978]. Examples of this type of model include the SPCTRAL2 model [*Bird and Riordan*, 1986] and the SMARTS2 model [*Gueymard*, 1995]. SPCTRAL2, SMARTS2, and other models can simulate solar irradiance under cloud-free conditions over specific discrete wavelength bands or integrated across the full spectrum. The models are semiempirical and, as with all clear-sky models, their performance relies heavily on the accuracy of input parameters [*Utrillas et al.*, 1998;

[1]Department of Geography, University of Hawai'i at Mānoa, Honolulu, Hawaii, USA.


0148-0227/12/2011JD016388

*Foyo-Moreno et al.*, 2000; *Tadros et al.*, 2005]. SPCTRAL2 and SMARTS2 have been tested and compared in several contexts. In general, both have proven versatile and accurate [*Gueymard*, 2001; *Jacovides et al.*, 2004]. In direct comparisons, SMARTS2 results have been somewhat better [*Utrillas et al.*, 1998], with results varying according to the spectral band of interest [*Foyo-Moreno et al.*, 2000; *Alados et al.*, 2002; *Tadros et al.*, 2005]. *Ineichen* [2006] emphasizes model selection should be based on simplicity of implementation and availability of input parameters. Because of our familiarity with the SPCTRAL2 model, having used it previously [*Nullet and Giambelluca*, 1992; *Larkin*, 2002], we elected to adopt it for use in this study.

[4] To produce estimates of clear sky radiation, these models have two primary tasks: accurately predicting the cosine-adjusted extraterrestrial radiation (ETR) reaching the Earth, and estimating the attenuation of incoming shortwave radiation as a function of optical path length and atmospheric optical properties. ETR and optical path length, determined by location on the Earth's surface, time of day and time of year, the geometry and timing of Earth's rotation, orbit, and the variation in the angle between the Earth's rotational axis and the plane of the ecliptic, are well simulated in clear-sky models. Variation in prediction skill is mainly associated with how well atmospheric transmission is simulated. Most applications of SPCTRAL2 and other clear-sky models focus on selection of atmospheric transmission parameter values appropriate for the study site. Temporal variations in atmospheric transmissivity resulting from day-to-day, seasonal, and interannual fluctuations in column water vapor, ozone, or aerosol loading have only rarely been considered in clear-sky model applications [cf. *Batlles et al.*, 2000; *Olmo et al.*, 2001; *Ineichen*, 2006]. With only limited prior research on this topic, a question remains as to the extent of uncertainty in modeled clear sky radiation resulting from the use of site specific, but temporally invariant atmospheric transmission parameter values.

[5] The primary objective of this study is to determine how results of a clear sky solar radiation model vary according to the use of several different input parameter schemes, representing a range of different levels of temporal resolution in atmospheric parameter settings, at sites on the Islands of Hawai'i and Maui, Hawai'i. Atmospheric transmissivity over Hawai'i varies day-to-day in response to fluctuating emission and transport of aerosols from local volcanic eruptions [*Smirnov et al.*, 2002] and distant sources of dust and pollution, varying marine aerosol production associated with breaking waves [*Porter et al.*, 2003], and variation in atmospheric humidity accompanying air mass changes. Annual cycles are seen in aerosols, with a February–June maximum associated with the period of active transport of Asian desert dust and pollution [*Holben et al.*, 2001; *Eck et al.*, 2005], and humidity, whose annual cycle is influenced by sea surface and air temperature.

[6] In this study, SPCTRAL2 model predictions integrated over the full solar spectrum (300–4000 nm) are compared against hourly global solar radiation measured under cloud free conditions. The SPCTRAL2 model has been shown to be adequate in prior studies using fixed parameter settings [*Nullet and Ekern*, 1988; *Foyo-Moreno et al.*, 2000; *Alados et al.*, 2002; *Jacovides et al.*, 2004]. Using time-varying (daily), broadband atmospheric input parameters from observations near the highest and lowest elevations in Hawai'i and interpolating them to intervening locations, we implement SPCTRAL2 for stations at a range of elevations. We evaluate model simulation of solar radiation and atmospheric transmissivity in relation to observations at each site and compare performance for model runs driven by daily, monthly, and 1 year mean atmospheric parameter settings. With high temporal resolution (daily) parameter values, the model should be able to simulate day-to-day variations in atmospheric transmissivity associated with fluctuations in aerosol amount and type and column water vapor. Using mean monthly settings will allow the model to capture the effects of annual cycles in aerosol concentration and water vapor content. While we test only the SPCTRAL2 model, we believe the results will be relevant to other models as well.

## 2. Methodology

### 2.1. SPCTRAL2 Model

[7] *Bird* [1984] proposed a simple model based on parametric methods previously developed by *Leckner* [1978] and *Brine and Iqbal* [1983]. SPCTRAL2 was developed by *Bird and Riordan* [1986] following improvements to Bird's original model by *Justus and Paris* [1985]. Required input parameters include local geographic coordinates, atmospheric pressure (P), precipitable atmospheric water vapor content (PW), aerosol optical depth (AOD), Ångström exponent ($\alpha$), surface albedo (A), and ozone concentration ($O_3$). Other factors that influence aerosol attenuation, i.e., forward scattering component (FC), aerosol single scattering albedo ($\omega_o$), aerosol asymmetry factor ($\cos\theta$), and the single scattering albedo at 400 nm ($\omega_{04}$) are generally held constant at default values. The model uses extraterrestrial spectral irradiance values for 122 wavelengths in the range of 300–4000 nm selected from the 10 nm resolution data set of (C. Fröhlich and C. Wehrli, World Radiation Center, personal communication, 1981) (as cited in the work of *Bird and Riordan* [1986]), much of which is derived from the spectrum of *Neckel and Labs* [1981]. Details of the SPCTRAL2 model are given by *Bird and Riordan* [1986]. The model is available online in several computer programming languages (available at http://rredc.nrel.gov/solar/models/spectral/SPCTRAL2/).

### 2.2. Atmospheric Transmission Parameters

[8] Natural and anthropogenic aerosols, water vapor, and other atmospheric gases determine the atmospheric transmission spectrum for solar radiation [*Myers et al.*, 2002]. SPCTRAL2 computes direct, spectrally resolved, normal-incidence radiation, $I_{d\lambda}$, using wavelength-dependent transmittance functions for Rayleigh scattering, aerosol attenuation, water vapor absorption, ozone absorption, and absorption by uniformly mixed gases [*Bird and Riordan*, 1986, equation (1)] as,

$$I_{d\lambda} = H_{0\lambda} D T_{r\lambda} T_{a\lambda} T_{w\lambda} T_{o\lambda} T_{u\lambda}, \quad (1)$$

where $H_{0\lambda}$ is ETR for a given wavelength, $\lambda$, estimated for the Earth's mean distance from the sun; $D$ is a factor for that corrects for variation in the Earth-Sun distance; and $T_{r\lambda}$, $T_{a\lambda}$, $T_{w\lambda}$, $T_{o\lambda}$ and $T_{u\lambda}$ are wavelength-dependent atmospheric transmittance functions for Rayleigh scattering, aerosol

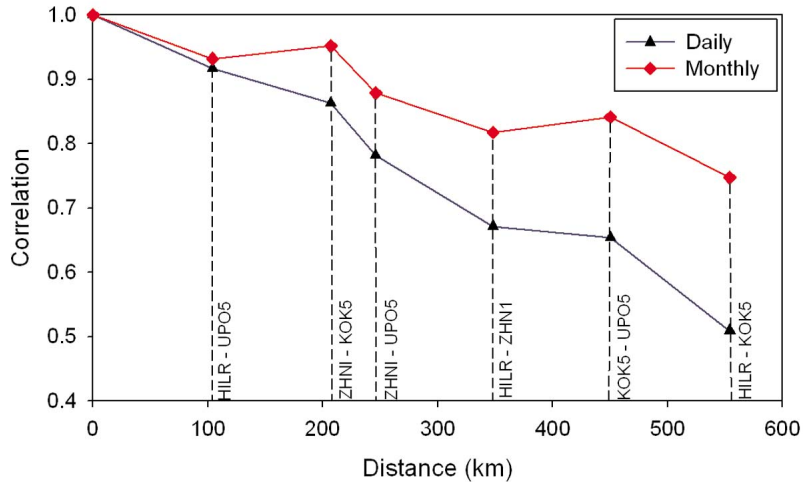


**Figure 1.** Correlation versus distance between stations for mean daily and mean monthly PW derived from GPSMET data for four near-sea level stations; HILR (Hilo, Hawai'i Island, 16 m), KOK5 (Kokele point, Kaua'i, 7 m), UPO5 (Upolo point, Hawai'i Island, 60 m), ZHN1 (Honolulu, O'ahu, 8 m).

attenuation, and absorption by water vapor, ozone, and mixed gases, respectively. The result of equation (1) is then adjusted by a factor of cos($\gamma$), where $\gamma$ is the solar zenith angle, to obtain radiation incident on a horizontal surface.

#### 2.2.1. Aerosol Optical Depth and the Ångström Exponent

[9] Atmospheric aerosols attenuate incoming shortwave radiation through absorption and scattering. Under cloud free conditions aerosol loading in the atmosphere is a major determinant of solar irradiance reaching the surface [*Olmo et al.*, 2001; *Alados et al.*, 2002; *Ineichen*, 2006]. Sources of aerosols include volcanic activity, sea salt, air pollution, and dust from deserts and agricultural activity. A quantitative measure of the total amount of aerosols between a point of observation and the top of the atmosphere is referred to as the Aerosol Optical Depth (AOD) [*Muller and Kong*, 2009]. Aerosol optical depth evaluated at a wavelength of 500 nm is used as a basic input parameter for the SPCTRAL2 model.

[10] The Ångström parameter, or wavelength exponent, ($\alpha$) is related to aerosol particle size distribution and controls the wavelength dependence of the effect of AOD on attenuation. When direct measurements of the Ångström wavelength exponent are not available, *Bird and Riordan* [1986] recommend using a value of 1.14. This value, however, may not be appropriate for optical environments where aerosols size may demonstrate significant variability, depending on the combination of anthropogenic and natural factors that influence their formation [*Dubovik et al.*, 2002]. *Holben et al.* [2001] showed that monthly mean $\alpha$ values ranged

**Table 1.** Site Characteristics and Mean Monthly and Annual Optical Conditions at Experimental Stations[a]

| | MLO | | | | HN-152 | | | HN-106 | | | HN119 | | | ALL |
|---|---|---|---|---|---|---|---|---|---|---|---|---|---|---|
| Elev (m) | 3397 | | | | 2590 | | | 1640 | | | 960 | | | |
| Press (mb) | 680 | | | | 747 | | | 835 | | | 905 | | | |
| Albedo | 0.05 | | | | 0.08 | | | 0.13 | | | 0.14 | | | |
| | MLO | | | | HN-152 | | | HN-106 | | | HN-119 | | | |
| Month | AOD | $\alpha$ | PWA | PWR | AOD | $\alpha$ | PWI | AOD | $\alpha$ | PWI | AOD | $\alpha$ | PWI | $O_3$ |
| Jul. 1999 | 0.010 | 0.90 | 0.19 | 0.41 | 0.014 | 0.82 | 0.60 | 0.021 | 0.72 | 1.10 | 0.029 | 0.61 | 1.82 | 0.267 |
| Aug. 1999 | 0.009 | 1.10 | 0.28 | 0.30 | 0.013 | 1.01 | 0.53 | 0.021 | 0.91 | 1.20 | 0.031 | 0.79 | 2.02 | 0.264 |
| Sep. 1999 | 0.008 | 0.85 | 0.21 | 0.25 | 0.011 | 0.84 | 0.48 | 0.018 | 0.79 | 1.08 | 0.026 | 0.76 | 1.81 | 0.265 |
| Oct. 1999 | 0.005 | 1.00 | 0.26 | 0.25 | 0.009 | 0.93 | 0.50 | 0.015 | 0.82 | 0.90 | 0.023 | 0.70 | 1.62 | 0.261 |
| Nov. 1999 | 0.012 | 1.21 | 0.24 | 0.21 | 0.015 | 0.98 | 0.46 | 0.023 | 0.76 | 0.92 | 0.032 | 0.55 | 1.55 | 0.257 |
| Dec. 1999 | 0.009 | 0.78 | 0.27 | 0.31 | 0.013 | 0.72 | 0.53 | 0.023 | 0.64 | 1.01 | 0.035 | 0.57 | 1.69 | 0.250 |
| Jan. 2000 | 0.010 | 1.36 | 0.25 | 0.24 | 0.014 | 1.11 | 0.43 | 0.021 | 0.87 | 0.91 | 0.030 | 0.66 | 1.51 | 0.258 |
| Feb. 2000 | 0.021 | 1.74 | 0.20 | 0.23 | 0.031 | 1.65 | 0.41 | 0.045 | 1.34 | 0.70 | 0.062 | 1.07 | 1.24 | 0.267 |
| Mar. 2000 | 0.019 | 1.08 | 0.22 | 0.28 | 0.025 | 0.96 | 0.45 | 0.038 | 0.85 | 0.90 | 0.053 | 0.74 | 1.55 | 0.273 |
| Apr. 2000 | 0.034 | 1.12 | 0.24 | 0.27 | 0.041 | 1.00 | 0.42 | 0.053 | 0.89 | 0.85 | 0.065 | 0.77 | 1.48 | 0.288 |
| May 2000 | 0.017 | 1.02 | 0.35 | 0.47 | 0.024 | 0.96 | 0.66 | 0.039 | 0.88 | 1.11 | 0.057 | 0.78 | 1.76 | 0.278 |
| Jun. 2000 | 0.014 | 1.03 | 0.24 | 0.29 | 0.019 | 0.95 | 0.52 | 0.028 | 0.86 | 1.10 | 0.040 | 0.75 | 1.80 | 0.271 |
| Annual | 0.014 | 1.10 | 0.25 | 0.29 | 0.019 | 0.99 | 0.50 | 0.029 | 0.86 | 0.98 | 0.040 | 0.73 | 1.66 | 0.267 |

[a]AOD is the aerosol optical depth, $\alpha$ is the angstrom exponent, PWA is AERONET derived precipitable water (cm), PWR is radiosonde derived precipitable water (cm), PWI is Interpolated radiosonde derived precipitable water (cm), $O_3$ is the ozone concentration (atm-cm): The same ozone values were used for all experimental sites.

**Table 2.** Statistical Results for SPCTRAL2 Modeled Versus Measured Solar Radiation at Mauna Loa Observatory[a]

| Run # | AOD | $\alpha$ | $O_3$ | PW | b | $r^2$ | MBE (W m$^{-2}$) | RMSE (W m$^{-2}$) | MBD (%) | RMSD (%) | MEAN (W m$^{-2}$) |
|---|---|---|---|---|---|---|---|---|---|---|---|
| Meas. | | | | | | | | | | | 888 |
| 1 | D | D | D | D-A | 0.978 | 0.997 | −10 | 17 | −1 | 2 | 879 |
| 2 | D | D | D | D-R | 0.978 | 0.992 | −17 | 27 | −2 | 3 | 871 |
| 3 | Y | D | D | D-A | 0.987 | 0.997 | −10 | 17 | −1 | 2 | 878 |
| 4 | Y | D | D | D-R | 0.978 | 0.992 | −18 | 28 | −2 | 3 | 871 |
| 5 | D | Y | D | D-A | 0.987 | 0.997 | −10 | 17 | −1 | 2 | 879 |
| 6 | D | Y | D | D-R | 0.978 | 0.992 | −17 | 27 | −2 | 3 | 871 |
| 7 | D | D | Y | D-A | 0.987 | 0.997 | −10 | 17 | −1 | 2 | 879 |
| 8 | D | D | Y | D-R | 0.978 | 0.992 | −17 | 27 | −2 | 3 | 871 |
| 9 | D | D | D | Y-A | 0.978 | 0.995 | −18 | 25 | −2 | 3 | 871 |
| 10 | D | D | D | Y-R | 0.973 | 0.995 | −22 | 29 | −2 | 3 | 866 |
| 11 | M | M | M | M-A | 0.980 | 0.995 | −16 | 24 | −2 | 3 | 872 |
| 12 | M | M | M | M-R | 0.973 | 0.994 | −22 | 30 | −2 | 3 | 866 |
| 13 | Y | Y | Y | Y-A | 0.978 | 0.995 | −18 | 25 | −2 | 3 | 870 |
| 14 | Y | Y | Y | Y-R | 0.973 | 0.995 | −23 | 29 | −2 | 3 | 866 |

[a]Under the AOD, $\alpha$, $O_3$ and PW columns, D indicates the use of measured AERONET time series as input, Y indicates use of a constant value equal to the 1 year measured mean, M indicates monthly measured mean, A indicates use of measured AERONET values time series for PW, R indicates use of measured Hilo Radiosonde to estimate the time series of PW. In the table headings, b is the slope of the linear least squares regression line with a zero intercept (observed = b * modeled), $r^2$ is the coefficient of determination, and MBE, RMSE, MBD, and RMSD are as defined in equations (4)–(7).

from 0.09 to 1.88 among the 21 AERONET stations used in their analysis.

[11] Daily observations of both AOD (evaluated at 500 nm) and $\alpha$ (evaluated at 440–870 nm) were retrieved from the NASA Goddard Space Flight Center Aerosol Robotic Network (AERONET) online data access system (http://aeronet.gsfc.nasa.gov/new_web/networks.html, accessed 24 March 2011). Each AERONET site employs a CIMEL sun/sky radiometer to measure solar extinction at 8 wavelengths, which are subsequently used to compute wavelength-specific AOD and $\alpha$ [*Holben et al.*, 2001]. These instruments are typically recalibrated approximately every ~3 months and have uncertainties of ~0.2 to 0.5% [*Holben et al.*, 1998]. CIMEL Sun photometers have been used at two AERONET sites in Hawai'i, Mauna Loa Observatory (MLO) at 3397 m elevation on the island of Hawai'i (19° 32′ 11″ N, 155° 34′ 37″ W) and a site at 20 m elevation on the island of Lāna'i (20° 44′ 06″ N, 156° 55′ 19″ W). The two sites are located near the highest (4205 m) and lowest (sea level) points in Hawai'i and are separated horizontally by only 193 km. Therefore, we can assume that differences in aerosol observations at these two sites are mainly representative of the altitude difference [*Eck et al.*, 2005]. Based on previous studies [*Porter et al.*, 2003; *Clarke and Kapustin*, 2010], we postulate that the vertical profiles of AOD and $\alpha$ in Hawai'i can be approximated by an exponential function fit to the observed values at the MLO and Lāna'i stations. This approach allows estimation of daily AOD and $\alpha$ values at intervening elevations during the period that the Lāna'i station was in operation (July 1996 to March 2004, with several long gaps). AOD scale height during that period averaged 2.24 ± 1.44 km.

[12] Many authors have stressed the necessity of choosing an appropriate aerosol parameterization in order to get accurate results using clear sky radiation models [*Utrillas et al.*, 1998; *Alados et al.*, 2002]. When site-specific aerosol optical measurements were not available, previous studies employing SPCTRAL2 have incorporated the use of different aerosol models (sets of parameter values), representing, for example, urban areas with varying degrees of air pollution [*Utrillas et al.*, 1998; *Foyo-Moreno et al.*, 2000; *Jacovides et al.*, 2004]. In general, this approach uses constant values of AOD and the Ångström exponent, and hence temporal fluctuations in the aerosol load and size spectrum are not represented. In this study, we are seeking to determine the added value of using time-dependent measurements of these input parameters.

### 2.2.2. Precipitable Water

[13] Precipitable water (PW) is the total water vapor content within the vertical column of air above a particular site expressed as the equivalent depth of liquid water (m), defined as,

$$PW = \frac{1}{\rho g} \int_{P_{top}=0}^{P_z} q dP, \tag{2}$$

where $\rho$ is the density of water (kg m$^{-3}$), g is gravitational acceleration (m s$^{-2}$), q is the specific humidity (kg kg$^{-1}$), P is the elevation-dependent atmospheric pressure (kg s$^{-2}$ m$^{-1}$), and the integral is evaluated from top of the atmosphere to the pressure level of the site. PW can be obtained from optical measurements of the atmospheric column with a Sun photometer [*Holben et al.*, 2001], or by integrating vertical humidity profile measurements.

[14] PW is highly variable in space and time in Hawai'i, with a large day-to-day variability and seasonal trends that show higher values in the summer and fall [*Holben et al.*, 2001]. The vertical distribution of water vapor is not uniform and is often characterized by a sharp discontinuity at the height of the trade-wind inversion [*Cao et al.*, 2007]. Given the complexity of the vertical profile, estimating PW along the study gradient based on AERONET measurements at MLO and Lāna'i was not considered to be an effective approach. Instead, the vertical humidity profiles taken at the Hilo radiosonde station (19.72°N 155.05°W) on the Island of Hawai'i were integrated to obtain PW at the elevation of MLO and each HaleNet station. The Hilo radiosonde station is approximately 58 km away from MLO and 167 km away from the HaleNet stations analyzed in this study. Note that

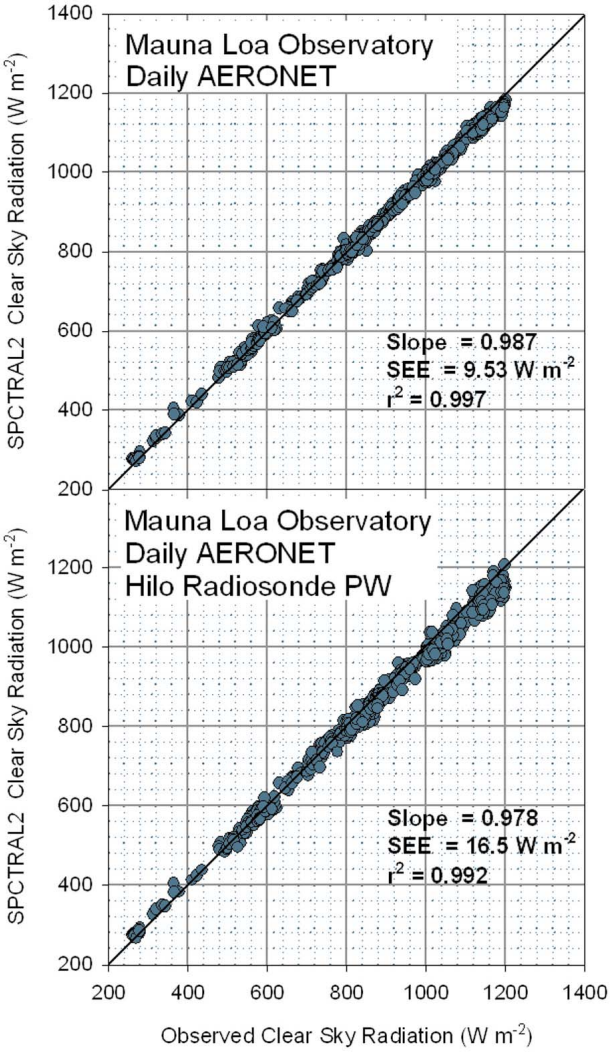


**Figure 2.** Comparison of SPCTRAL2 clear sky solar radiation estimates using aerosol input parameters obtained from AERONET measurements at Mauna Loa Observatory with observed solar radiation on clear days at MLO; precipitable water (PW) derived from (top) AERONET and (bottom) Hilo radiosonde profiles.

radiosonde humidity measurements are subject to several sources of error, most significantly sensor hysteresis, which affects sensors under high humidity followed by low humidity; these errors may exceed 10% relative humidity [*Blackmore and Taubvurtzel*, 1999]. At MLO, both the AERONET-observed PW and that derived from the radiosonde profile were tested. Using discrete observations of specific humidity ($q_i$) and pressure ($P_i$) along a vertical profile (levels $i$ = 1,n), PW was estimated for a site at any given pressure level, $P_z$, between the $k$th and $k$ + 1st observation levels as,

$$PW = ab + \frac{1}{2}ac + \sum_{i=k+1}^{n} d_i e_i + \frac{1}{2} d_i f_i, \qquad (3)$$

where, for $P_{i=k} > P_z > P_{i=k+1}$, $q_z = q_{i=k+1} + \left[ \frac{q_{i=k} - q_{i=k+1}}{P_{i=k} - P_{i=k+1}} (P_z - P_{i=k+1}) \right]$, $a = P_z - P_{i=k+1}$, $b = \min(q_z, q_{i=k+1})$, $c = |q_z - q_{i=k+1}|$, $d = P_i - P_{i+1}$, $e = \min(q_i, q_{i+1})$, and $f = |q_i - q_{i+1}|$. Based on radiosonde-derived PW for an 812 day sample period (between November 2004 and February 2007), PW scale height averaged 1.58 ± 0.40 km.

### 2.2.3. Ozone and Other Input Parameters

[15] The majority of ozone absorption takes place in the stratosphere [*Gueymard*, 2003a], with only a small additional amount of absorption by tropospheric ozone. Using a broadband radiation model, *Ineichen* [2006] showed that even large variations in column ozone concentration resulted in very small changes in clear sky radiation. The ozone optical depth used in this study was computed using the determinations of total ozone columnar concentration from data obtained from a Dobson Ozone Spectrometer operated by the National Oceanic and Atmospheric Administration at MLO (National Oceanic and Atmospheric Administration (NOAA), Earth System Research Laboratory Global Monitoring division, 2011, available at http://www.esrl.noaa.gov/gmd/ozwv/). Of the total column ozone in Hawai'i, NOAA (online, 2011) reported an average of 7 Dobson Units (DU) of ozone in the troposphere. Given the relatively low proportion of ozone there, variations in the tropospheric ozone were considered to have a negligible effect on absorption. Therefore, we used MLO measured ozone values for all sites, with no adjustment for elevation.

[16] Air pressure was held constant at each station at a value estimated as a function of elevation using the hypsometric equation. Surface albedo values were determined based on field observations at each HaleNet station. Geographic coordinates were established with a GPS unit at each station.

### 2.2.4. Horizontal Variability in Atmospheric Optical Properties

[17] In this study, we implicitly assume that horizontal variations in daily, monthly mean, and 1 year mean optical parameter values are negligible within the domain of the experimental sites. Transient horizontal gradients in column water vapor can occur during the passage of weather disturbances, and gradients in aerosol load can persist in areas affected by sea spray and volcanic emissions. However, we believe these effects to be minimal for the sites in this study. Analysis of data from the NOAA Ground-Based GPS Meteorology Web site (available at http://www.gpsmet.noaa.gov/), which includes eight sites with PW in Hawai'i, demonstrates that column water vapor varies mainly according to elevation. On daily, monthly, and long-term mean intervals, horizontal differences are very small in comparison with vertical differences, despite large differences in mean annual precipitation (MAP) (T. W. Giambelluca et al., The rainfall atlas of Hawai'i, 2011, available at http://rainfall.geography.hawaii.edu) among the sites. For example, period-of-record PW averages, derived from GPSMET data for the four near-sea level stations are 3.21 cm for Hilo, Hawai'i Island (MAP = 3244 mm), 2.99 cm for Upolu Point, Hawai'i Island (MAP = 807 mm), 2.97 cm for Honolulu, O'ahu (MAP = 563 mm), and 3.01 cm for Kokole Point, Kaua'i (MAP = 459 mm). The range of these values, 0.24 cm, is less than 8% of the mean Hilo value, despite a sevenfold

**Table 3.** Statistical Results for SPCTRAL2 Modeled Radiation Divided by ETR Versus Measured Solar Radiation Divided by ETR at Mauna Loa Observatory[a]

| Run # | AOD | $\alpha$ | $O_3$ | PW | a | b | $r^2$ | MBE | RMSE | MBD (%) | RMSD (%) | MEAN |
|---|---|---|---|---|---|---|---|---|---|---|---|---|
| Meas. | | | | | | | | | | | | 0.881 |
| 1 | D | D | D | D-A | 0.284 | 0.669 | 0.892 | −0.008 | 0.016 | −1 | 2 | 0.874 |
| 2 | D | D | D | D-R | 0.349 | 0.587 | 0.674 | −0.015 | 0.024 | −2 | 3 | 0.867 |
| 3 | Y | D | D | D-A | 0.268 | 0.687 | 0.900 | −0.008 | 0.015 | −1 | 2 | 0.873 |
| 4 | Y | D | D | D-R | 0.333 | 0.605 | 0.683 | −0.015 | 0.024 | −2 | 3 | 0.866 |
| 5 | D | Y | D | D-A | 0.283 | 0.670 | 0.892 | −0.008 | 0.016 | −1 | 2 | 0.874 |
| 6 | D | Y | D | D-R | 0.348 | 0.589 | 0.675 | −0.015 | 0.024 | −2 | 3 | 0.867 |
| 7 | D | D | Y | D-A | 0.280 | 0.673 | 0.894 | −0.008 | 0.015 | −1 | 2 | 0.874 |
| 8 | D | D | Y | D-R | 0.346 | 0.592 | 0.677 | −0.015 | 0.024 | −2 | 3 | 0.867 |
| 9 | D | D | D | Y-A | 0.342 | 0.595 | 0.822 | −0.015 | 0.023 | −2 | 3 | 0.866 |
| 10 | D | D | D | Y-R | 0.331 | 0.602 | 0.822 | −0.015 | 0.027 | −2 | 3 | 0.861 |
| 11 | M | M | M | M-A | 0.336 | 0.603 | 0.808 | −0.014 | 0.022 | −2 | 3 | 0.867 |
| 12 | M | M | M | M-R | 0.380 | 0.546 | 0.762 | −0.020 | 0.027 | −2 | 3 | 0.862 |
| 13 | Y | Y | Y | Y-A | 0.321 | 0.618 | 0.820 | −0.016 | 0.023 | −2 | 3 | 0.865 |
| 14 | Y | Y | Y | Y-R | 0.625 | 0.625 | 0.820 | −0.021 | 0.026 | −2 | 3 | 0.860 |

[a]All symbols are the same as in Table 2. The regression in this case was not forced through the origin, hence, the y-intercept (a) is given.

difference in MAP between the driest and wettest sites. Correlation among sea level sites for PW at daily and monthly intervals is high for stations within 200 km of each other (Figure 1). Note that all study sites are within 160 km of the Hilo radiosonde station. The horizontal differences in sea level PW, though small, are likely to be greater than those at higher elevations. The influences of topography and land-ocean thermal contrasts that give rise to modest horizontal humidity gradients near sea level diminish with elevation. Therefore, it is likely that horizontal differences are much smaller at the elevations of MLO and the HaleNet stations analyzed in our study.

### 2.3. Solar Radiation Observations

#### 2.3.1. Solar Radiation Observation Sites

[18] To test the model, results were compared with solar radiation measurements taken on clear days. We used observed solar radiation from four sites, Mauna Loa Observatory (MLO) at 3397 m elevation on the island of Hawai'i (19.53°N, 155.57°W), and three of the eleven stations making up the HaleNet Climate Network on the slopes of Haleakalā Volcano Maui, Hawai'i (http://climate.socialsciences.hawaii.edu/HaleNet/Index.htm). MLO, best known as the site of the longest continuous observations of atmospheric $CO_2$, is one of the premier climate monitoring sites in the world. In addition to the AERONET observations mentioned previously, measurements taken at MLO include incident radiation on a horizontal surface measured with an Eppley PSP precision pyranometer (Eppley Laboratory, Newport, RI, USA). The Eppley PSP has a calibration uncertainty of 2 to 3% [*Riihimaki and Vignola*, 2008] and may experience a thermal offset of $-30$ W m$^{-2}$ to $-5$ W m$^{-2}$ [*Reda et al.*, 2003]. The three HaleNet stations used in this study are located on the leeward side of the island of Maui at elevations ranging from 960 to 2590 m. Each of the three stations is equipped with an Eppley 8–48 pyranometer measuring global solar radiation, sampled at a 10 s interval and recorded hourly using a Campbell Scientific, Inc. (Logan, UT, USA) CR10X data logger. The Eppley model 8–48 has a cosine response of ±2% (Eppley Laboratory Inc., Instrumentation for the measurement of the components of solar and terrestrial radiation, Newport, R. I.) and has been shown to exhibit a low thermal offset (±1 W m$^{-2}$) [*Reda et al.*, 2003]. The SPCTRAL2 model was run separately for each of the four stations, with geographic coordinates, pressure, atmospheric absorption and scattering parameters, and albedo set to represent each site. Fixed parameter values as well as monthly and 1 year average optical conditions for each site are given in Table 1.

[19] Model results were compared with clear sky measurements during the 1 year time period 1 July 1999 through 30 June 2000. This time period was selected because it follows the deployment at all HaleNet stations of Eppley pyranometers in July 1999 immediately after they were calibrated. For consistency, the same 1 year period was used for testing at the MLO site.

#### 2.3.2. Sensor Intercalibration

[20] In June 1999, nine Eppley 8–48 pyranometers were mounted in close proximity to each other at a field research area on the University of Hawai'i at Mānoa campus. Sensors were sampled at a 10 s interval and recorded hourly over a period of 6 days. Of the nine, five were newly calibrated at Eppley Laboratory. At each time interval, the mean of the recently calibrated sensors was calculated and used as a standard for comparison with the four remaining sensors. The slope of the least squares linear regression, with a forced zero intercept, between the sensor and the standard was used to adjust the calibration factor of each sensor. After adjustment, standard errors of each of the nine sensors in relation to the mean of the recently calibrated sensors were between 3 and 6 W m$^{-2}$. Three of the nine sensors subjected to this intercalibration procedure were subsequently deployed to the three HaleNet stations used in this study.

#### 2.3.3. Identifying Clear Days

[21] Cloud screening methods have been developed that utilize visual cloud observations [*Alados-Arboledas et al.*, 2000, *Alados et al.*, 2002] or measurements of both global and diffuse solar radiation [*Long and Ackerman*, 2000]. These methods were not applicable for our study, because cloud observations and diffuse radiation measurements were not available at all sites. To identify whole clear days (0900 to 1700 HST) at the experimental stations, the difference between the modeled and measured radiation was taken for each of the eight hours of peak insolation. For each day, the

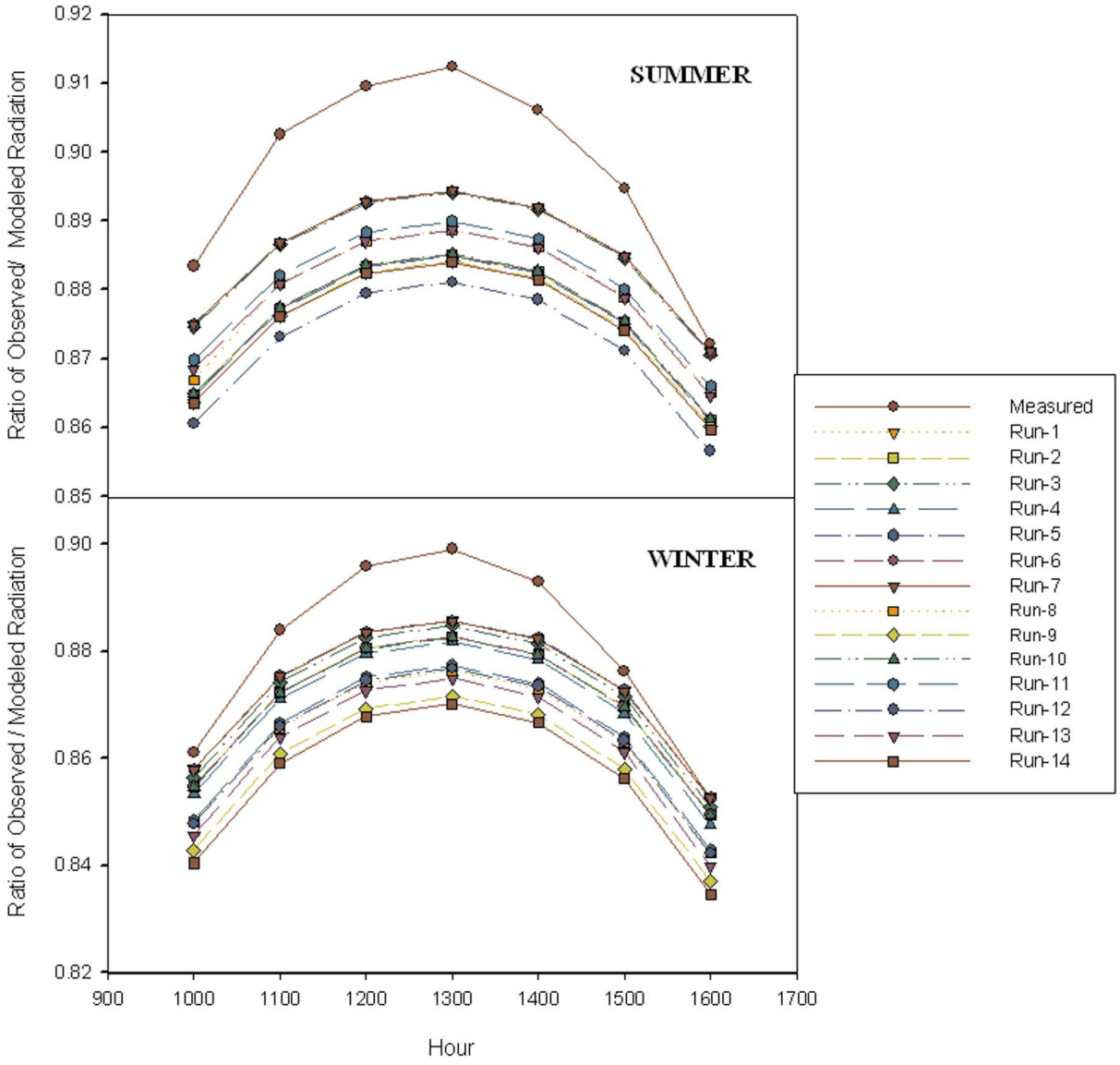


**Figure 3.** Mean diurnal variation in atmospheric transmissivity based on measured solar radiation during clear days at Mauna Loa Observatory and on SPCTRAL2 model runs using fourteen input schemes, during (top) summer and (bottom) winter periods. Individual means calculated from all values at a given hour with each season. Corresponding standard deviations are not shown to avoid crowding. Average standard deviations of individual hours for runs with daily PW (0.013, summer; 0.015 winter) were higher than for runs with monthly or yearly averaged PW (0.003, summer; 0.007 winter), and less than the standard deviations of measured transmissivity (0.014, summer; 0.021, winter).

standard deviation (SD) of the hourly model-observed difference was calculated. Days with low variability in the difference were chosen, using an arbitrarily selected criterion of SD < 13 W $m^{-2}$. Candidate clear days identified in this way were manually screened to ensure cloud free conditions. This method, which identified whole days with cloud-free conditions, was applied at all stations. However, a sufficient number of cloud free (CF) days were identified this way only at the MLO site (80 CF days). Located well above the mean trade wind inversion level, MLO experiences frequent cloud-free days. For the HaleNet stations, located at lower elevations with fewer whole clear days (e.g., HN-106, 11 CF days), an additional cloud screening method was applied to identify cloud-free periods within a given day. HaleNet solar radiation values were manually screened to select hours that followed a typical diurnal pattern under cloud free conditions. To accomplish this, solar radiation values for each day were plotted over the 8 h time period and only hours which followed the typical diurnal pattern under cloud free conditions were selected. Modeled clear sky radiation was used as a reference; clear hours measured radiation matched the shape of the modeled radiation time series. The difference between the modeled and measured radiation was not used as part of the selection criteria.

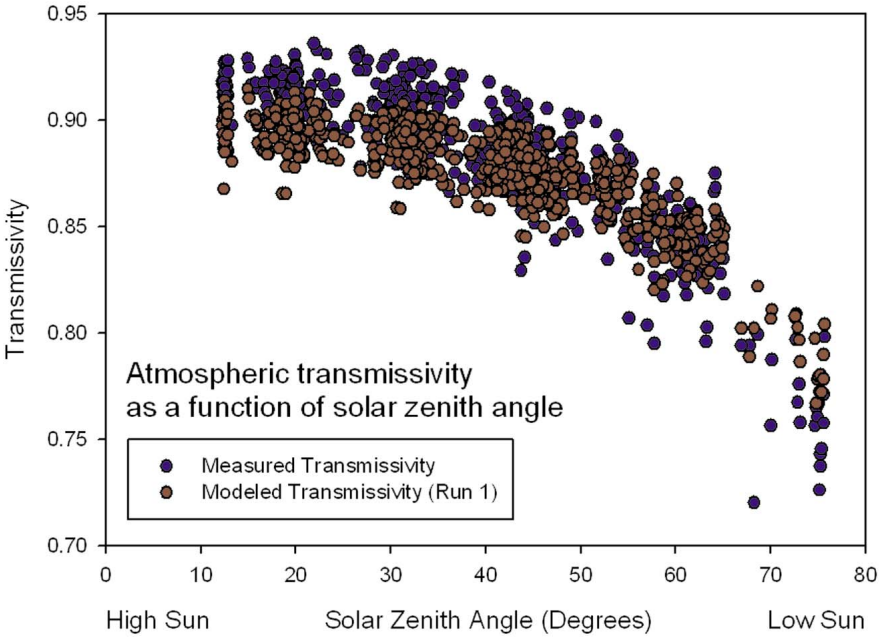


**Figure 4.** Modeled and measured atmospheric transmissivity as a function of solar zenith angle.

#### 2.3.4. Evaluating the Model

[22] The accuracy of the model was evaluated using Mean Bias Error (MBE) and Root Mean Square Error (RMSE). These statistical indicators are defined as:

$$\mathrm{MBE} = \sum_{i=1}^{N} \frac{(y_i - x_i)}{N} \tag{4}$$

$$\mathrm{RMSE} = \left\{ \frac{\sum_{i=1}^{N} (y_i - x_i)^2}{N} \right\}^{1/2}, \tag{5}$$

where N is the number of observations and $y_i$ is the predicted value and $x_i$ is the measured value. Alternatively, bias and random error can also be computed as the Mean Bias Deviation (MBD) and root-mean-square deviation (RMSD), expressed as a percentage [*Foyo-Moreno et al.*, 2000],

$$\mathrm{MBD} = \frac{1}{N} \sum_{i=1}^{N} \frac{y_i - x_i}{x_i} \times 100 \tag{6}$$

$$\mathrm{RMSD} = \left[ \frac{1}{N} \sum_{i=1}^{N} \left( \frac{y_i - x_i}{x_i} \right)^2 \right]^{1/2} \times 100. \tag{7}$$

[23] Linear regression between modeled and measured values was also computed. For the solar radiation analysis, the $y$ intercepts were negligibly different from zero (not shown). For simplicity, therefore, the regression lines for solar radiation were forced through the origin. However, for atmospheric transmission, the $y$ intercept values were significantly different from zero, and zero intercept was not forced.

## 3. Results and Discussion

### 3.1. Model Validation at MLO

[24] Model results were initially compared against solar radiation measurements at MLO. Because MLO conducts daily Sun photometer measurements of atmospheric transmissivity and upholds high standards for instrument calibration [*Eck et al.*, 2005], this site is ideal for applying SPCTRAL2. To determine the effects of using radiosonde-derived rather than AERONET-derived PW, and of using mean rather than time-dependent inputs, the model was implemented at MLO under 14 input parameter schemes (Table 2). Of the 80 CF days identified in the cloud screening process, 53 were chosen based on the fact that they represented days for which both AERONET- and Hilo-radiosonde-derived PW were available. Measured and modeled hourly solar radiation values were compared during the 53 days (584 h) of clear sky conditions between the hours of 0900 and 1700 (HST).

[25] Results indicate close agreement between estimated and measured solar radiation for all input schemes (Table 2). It should be noted that discrepancies between measured and modeled radiation are partly explained by measurement error. The model underestimated measured radiation by 1%–3% based on the slope, 10–23 W $m^{-2}$ based on MBE, or 1%–2% based on MBD. Random error was small at 17–30 W $m^{-2}$ RMSE or 2%–3% RMSD. Points fell close to the 1:1 line for each of the PW schemes (Figure 2). However, use of AERONET PW yielded consistently better results than Hilo radiosonde PW (Table 2). The model performed best when daily AERONET-derived values of

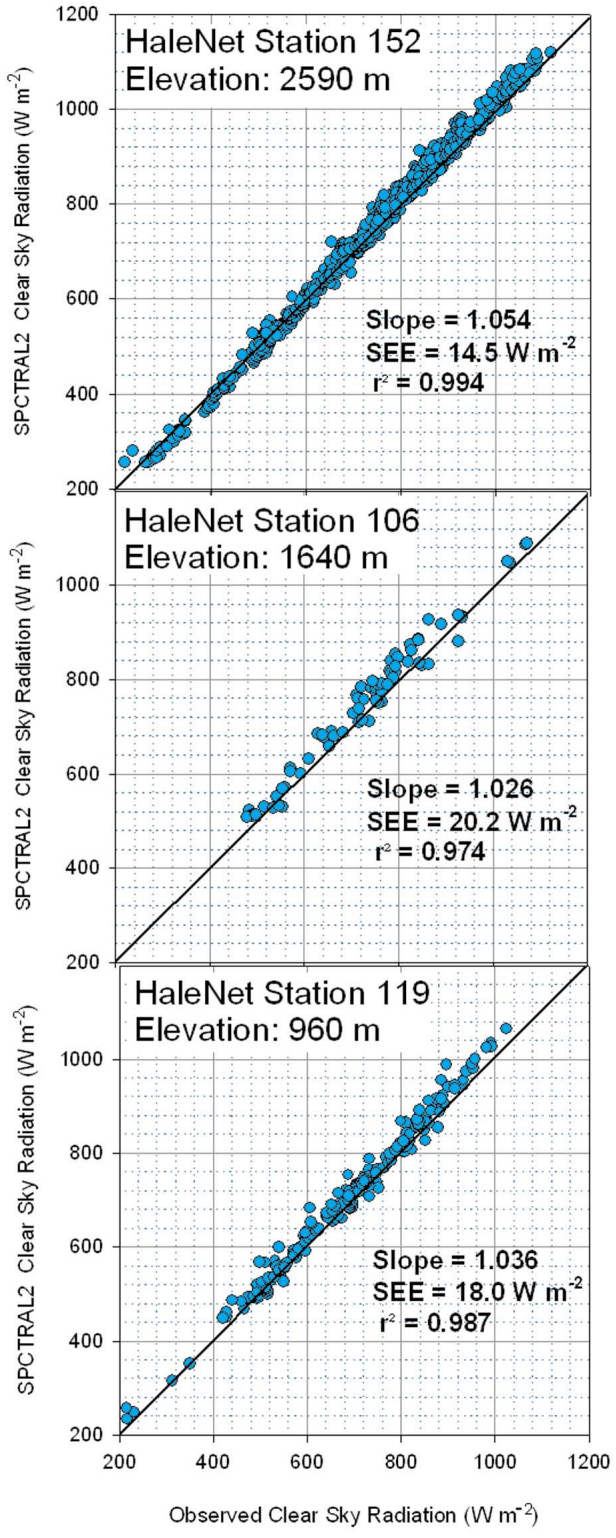


**Figure 5.** Comparison of SPCTRAL2 clear sky solar radiation estimates using fixed (1 year mean) parameter settings (scheme Y) with observed solar radiation clear days at HaleNet Stations (top) 152, (middle) 106, and (bottom) 119.

PW were used (Runs 1, 3, 5 and 7). Holding $\alpha$ constant at the 1 year mean value (Runs 5–6) had a negligible effect. AOD has a significant annual cycle, with February–June maximum [*Holben et al.*, 2001; *Eck et al.*, 2005] as is evident in the monthly AOD values presented in Table 1. However, holding AOD constant at the 1 year mean (Runs 3 and 4) did not have much effect on the outcome, increasing RMSE by less than 0.5 W $m^{-2}$. When PW was held constant (Runs 9 and 10) errors increased under both schemes.

[26] The results show that accurately representing daily variability in PW does benefit model performance. When all variables were held constant at their monthly mean or 1 year mean values under the radiosonde PW scheme, model bias and random error, although still reasonably low, were higher than all other model runs. On average monthly mean values of Hilo-radiosonde-derived PW were 0.04 $\pm$ 0.06 cm greater (Table 1) than the AERONET-derived PW. This explains the greater underestimation by the model when using PW-R. The comparison of the two sources for PW input suggests that data from a nearby radiosonde station can provide a good alternative when AERONET-derived PW measurements are not available. The MLO results also show that the temporal variability of AOD and $\alpha$ do not have a significant impact on model performance, suggesting that the use of constant site-specific parameter values are justified.

[27] The last four MLO model runs, with atmospheric variables set to their respective monthly (Runs 11 and 12) and 1 year (Runs 13 and 14) mean values, produced surprisingly good results. This indicates that the use of time-averaged parameter values causes only a relatively small degradation of model performance compared with results obtained with daily input data (Runs 1 and 2). ANOVA was used to test the differences among the results of the various model runs. Based on estimated hourly radiation, all runs were statistically similar to one another ($p = 0.05$). Similarly, for five broadband radiative transfer models, *Batlles et al.* [2000] found that the use of monthly averaged input parameter values, as opposed to hourly inputs, had negligible effects on global irradiance estimates for two stations in Spain.

[28] The generally good results obtained here for MLO are consistent with results of a study by *García et al.* [2008], who compared MLO broadband irradiance with modeled AERONET-derived broadband fluxes calculated using a spectral integration method. They obtained relatively small model errors for MLO (RMSE 9.5 W $m^{-2}$ and MBE 2 $\pm$ 10 W $m^{-2}$) compared with sites in their study with higher, more variable aerosol loads.

### 3.2. Modeled Atmospheric Transmission

[29] To obtain measurements and model estimates of atmospheric transmissivity, observed solar radiation and modeled results were divided by the cosine- and Earth-Sun-distance-adjusted ETR. Modeled transmissivity was tested in relation to measured values for all twelve model input schemes run at MLO (Table 3). Results follow a similar pattern to those obtained for solar radiation (Table 2), with all runs based on direct measurements of PW showing the lowest errors. In all runs, atmospheric transmissivity was underestimated, by 0.8–2.3% (MBD). ANOVA testing of transmissivity results confirmed that most runs using daily

**Table 4.** Statistical Results for SPCTRAL2 Modeled Versus Measured Solar Radiation at HaleNet Stations[a]

| Run | N | Elev. (m) | b | $r^2$ | MBE (W $m^{-2}$) | RMSE (W $m^{-2}$) | MBD (%) | RMSD (%) | MEAN (W $m^{-2}$) |
|---|---|---|---|---|---|---|---|---|---|
| 152-Measured | | | | | | | | | 761 |
| 152-D | 753 | 2590 | 1.054 | 0.994 | 18 | 25 | 2 | 3 | 779 |
| 152-M | 753 | 2590 | 1.054 | 0.994 | 10 | 20 | 1 | 3 | 772 |
| 152-Y | 753 | 2590 | 1.054 | 0.994 | 8 | 19 | 1 | 3 | 770 |
| 106-Measured | | | | | | | | | 733 |
| 106-D | 75 | 1640 | 1.037 | 0.968 | 28 | 38 | 4 | 5 | 762 |
| 106-M | 75 | 1640 | 1.03 | 0.974 | 23 | 32 | 3 | 4 | 756 |
| 106-Y | 75 | 1640 | 1.026 | 0.974 | 20 | 31 | 3 | 4 | 754 |
| 119-Measured | | | | | | | | | 681 |
| 119-D | 200 | 960 | 1.036 | 0.987 | 24 | 31 | 4 | 5 | 705 |
| 119-M | 200 | 960 | 1.029 | 0.987 | 20 | 27 | 3 | 4 | 701 |
| 119-Y | 200 | 960 | 1.036 | 0.987 | 17 | 26 | 2 | 4 | 698 |

[a]In the run names, D indicates runs with vertically interpolated, daily values for AOD, $\alpha$, and PW, with PW derived from Hilo radiosonde data; M indicates model runs using monthly mean values for AOD, $\alpha$ and PW; and Y indicates model runs with AOD, $\alpha$ and PW held constant at annual mean values.

PW were significantly different ($p = 0.05$) from runs using monthly or yearly averaged PW. Oddly, the exception to this was for daily radiosonde PW versus averaged AERONET PW, which were not significantly different. For runs involving daily PW, all with like PW source were not significantly different, and all with different PW sources were significantly different.

[30] Transmissivity was also assessed by averaging clear day measurements and modeled irradiance for each individual hour. Mean diurnal patterns calculated for summer

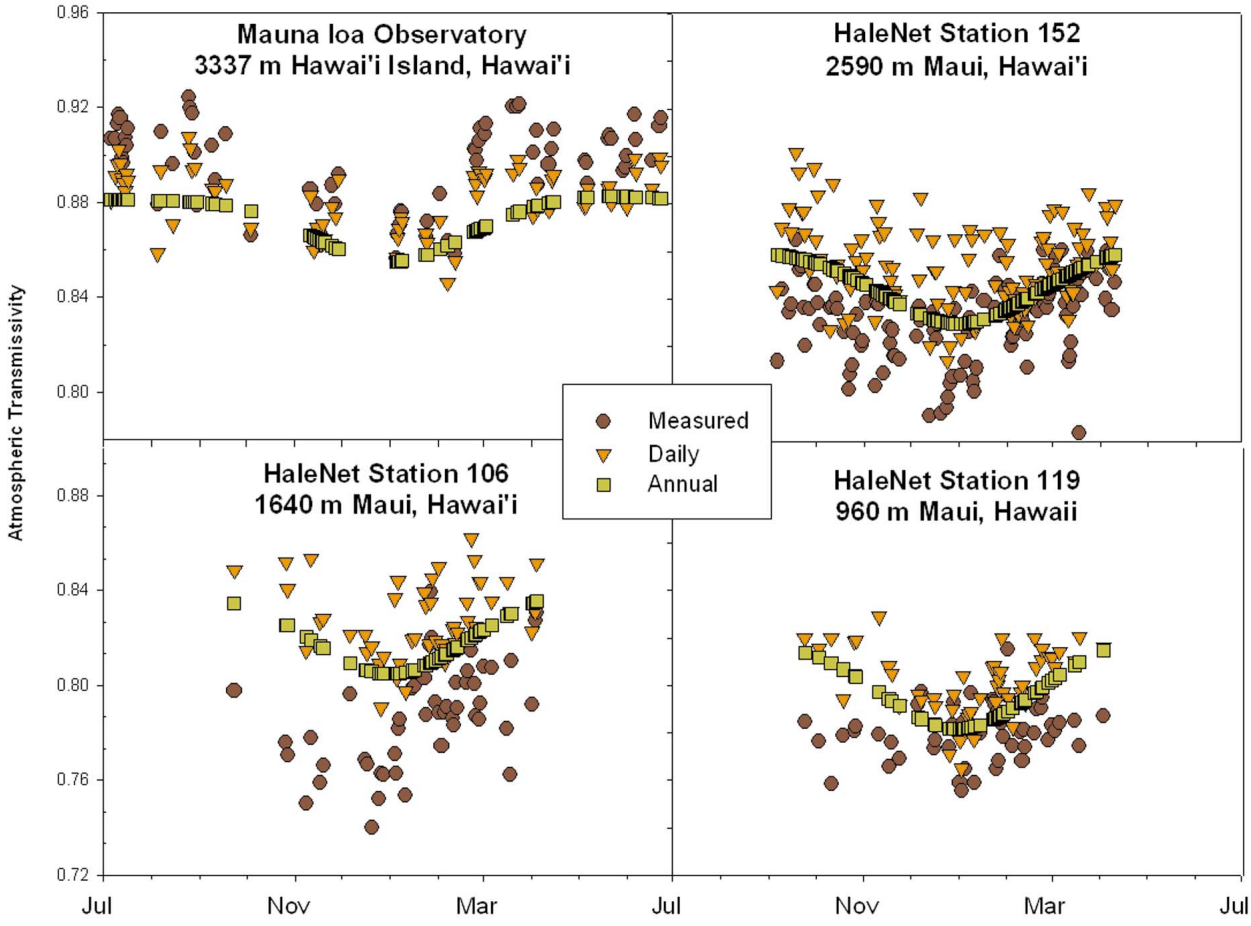


**Figure 6.** Comparison of measured and modeled atmospheric transmissivity at MLO (top left), HaleNet Station 152 (top right), Station 106 (bottom left), and Station 119 (bottom right). Modeled runs done with daily and 1 year mean input parameter setting.

**Table 5.** Model Parameter Values Used to Test Model Sensitivity to Temporal Variation in Optical Parameters[a]

| | MLO | | | Lāna'i | | |
|---|---|---|---|---|---|---|
| Parameter | AOD | $\alpha$ | PW | AOD | $\alpha$ | PW |
| Max. | 0.034 | 1.74 | 0.47 | 0.100 | 0.91 | 2.94 |
| Mean | 0.014 | 1.09 | 0.25 | 0.066 | 0.65 | 2.67 |
| Min. | 0.005 | 0.78 | 0.21 | 0.044 | 0.50 | 2.39 |

[a]Aerosol Optical Depth (AOD) at 500 nm, Angstrom exponent ($\alpha$) at 440–870 nm, precipitable water (PW) in cm.

(April–September) and winter (October–March) seasons (Figure 3) show that the underestimation of transmissivity is greatest for midday summer periods, suggesting that model error is sun-angle dependent. Plotting all clear sky observed and modeled (Run 1) transmissivity as a function of solar zenith angle (Figure 4) shows that for low zenith angle, i.e., for more vertical sun and minimum optical path length, model underestimation of atmospheric transmission is greatest, while for high zenith angle (low sun, long optical path length), the model overestimates transmissivity at MLO.

### 3.3. Model Application at HaleNet Stations

[31] The SPCTRAL2 model was applied at three HaleNet stations using three different input scenarios at each location: scheme (D) used daily input parameters derived from the methodology explained above in which AOD and $\alpha$ were interpolated from AERONET-measured values and Hilo radiosonde measurements were used for PW; scheme (M) set parameters to their respective monthly mean values; and scheme (Y) held all parameters constant at their respective 1 year mean values. Parameter values for schemes M and Y are presented Table 1. The time period 0900 to 1700 was used to avoid effects of topographical obstructions evident for early morning and late afternoon hours on the western slope of Haleakalā. Scatterplots of observed radiation versus radiation modeled with input parameters held constant (scheme Y) at the three HaleNet stations (Figure 5) show that the model performs very well. Table 4 summarizes the results for the three HaleNet stations. Again, we note that model-measurement discrepancies are partly explained by measurement error. The model tended to overestimate solar radiation at all stations under all three input schemes, but nevertheless produced satisfactory results with regression slopes all within 0.03 of unity and RMSE values in the range of 18.9–38.0 W $m^{-2}$. In terms of MBE, RMSD, and MBD, the model performed better at all three stations when scheme M or Y was implemented, i.e., when monthly or annual input parameters were used. The best performance was obtained by holding parameters constant at their annual mean values.

#### 3.3.1. Atmospheric Transmissivity at HaleNet Sites

[32] Modeled results at the MLO were improved when daily measurements (Runs 1–2) were used as opposed to monthly or annual parameter settings (Runs 9–12). The opposite result was obtained for the HaleNet stations. To assess why the model performed better at the HaleNet stations when inputs were held constant, atmospheric transmissivity was analyzed (Figure 6). Use of daily parameter values (Run 1) at MLO does well at capturing the day-to-day variability in the actual observed transmission, compared with using constant annual mean parameter values (Run 11), which resulted in under prediction of the observations. Use of daily parameter values at HaleNet stations obviously results in more day-to-day variability than simulations using constant annual mean parameter values. However, annual parameter settings produce results closer to the observations. This shows that it is preferable to use time-averaged atmospheric parameter values if time-variant values cannot be accurately estimated. Use of daily parameter values improved model performance only at MLO, where daily direct optical measurements of atmospheric variables are taken. However, MLO is hardly typical in this regard, as most sites of interest will not have the luxury of a colocated AERONET station. Despite being bracketed (vertically) by the MLO and Lāna'i AERONET stations and having a nearby radiosonde station at Hilo, interpolated aerosol parameters and radiosonde-derived PW used at the HaleNet stations in this study did not capture this day-to-day variation well and annual mean values of these parameters produced more accurate results.

[33] It should be noted that because of the isolation of Hawai'i from continental sources areas for desert dust and pollutants, the variability of atmospheric attenuation is relatively low there compared with other locations. Among 21 AERONET sites analyzed by *Holben et al.* [2001] with statistics over the complete annual cycle, MLO and Lāna'i had the lowest annual ranges of AOD and PW. To test the sensitivity of the model to observed ranges of the key atmospheric variables, we ran the model using the maximum, mean, and minimum of the mean monthly values of AOD, $\alpha$, and PW at both MLO and Lāna'i, (Table 5) while holding all other parameters at their mean monthly values. This was done for two sample days representing high and low sun conditions, 21 June and 21 December, respectively. The results, shown in terms of model-estimated transmissivity (Table 6), indicate only very small differences in atmospheric transmissivity due to variation in these parameters over the annual cycle. Variations in transmissivity are higher for AOD and PW than for $\alpha$, and are higher at Lāna'i than at MLO. But in all cases, these parameter shifts result in transmissivity changes of less than $\pm 1\%$. These relatively

**Table 6.** Mean Diurnal Model-Estimated Transmissivity Under Varying Input Scenarios[a]

| | MLO | | Lāna'i | |
|---|---|---|---|---|
| Runs | Jun | Dec | Jun | Dec |
| | | *AOD* | | |
| Max | 0.860 | 0.770 | 0.710 | 0.703 |
| Mean | 0.863 | 0.774 | 0.715 | 0.710 |
| Min | 0.864 | 0.776 | 0.718 | 0.715 |
| | | $\alpha$ | | |
| Max | 0.863 | 0.774 | 0.715 | 0.711 |
| Mean | 0.863 | 0.774 | 0.715 | 0.710 |
| Min | 0.863 | 0.773 | 0.714 | 0.709 |
| | | *PW* | | |
| Max | 0.859 | 0.770 | 0.710 | 0.706 |
| Mean | 0.863 | 0.774 | 0.715 | 0.710 |
| Min | 0.868 | 0.779 | 0.721 | 0.717 |

[a]The model was run using maximum, mean, and minimum values for AOD, $\alpha$, and PW during the year in question.

small variations in atmospheric transmission are most likely attributable to the low monthly mean values used in this sensitivity analysis. Overall variations in the annual cycle of atmospheric optical properties is generally low in Hawai'i when compared to other AERONET sites around the world [*Holben et al.*, 2001].

## 4. Conclusions

[34] Application of the SPCTRAL2 clear sky solar radiation model at MLO produced reasonably accurate estimates of solar radiation under all input parameter schemes. On average, atmospheric transmissivity at MLO was slightly underestimated (1–2%). Midday summer periods had the largest error, i.e., model underestimation of atmospheric transmissivity was greatest for a more vertical sun and minimum optical path length, while for low sun and greater optical path length the model slightly overestimated transmissivity. The model performed best when time-dependent AERONET-derived inputs were used and errors were higher when annual mean values and radiosonde-derived PW were used. Comparison of the two PW sources suggests that data obtained from a nearby radiosonde station can provide a good alternative when AERONET-derived PW measurements are not available. The results also show that the temporal variability of AOD and $\alpha$ did not have a significant impact on the model performance at MLO, indicating that constant site-specific parameter values can be used with relatively little degradation of model performance. However, it should be noted that the SPCTRAL2 model is considered to be rather simplistic, and hence, it is possible that more sophisticated clear-sky models may derive greater benefit from temporally resolved input data.

[35] Applying results from the model at three HaleNet stations across a 1630 m elevation gradient indicated overestimation of observed clear sky radiation. The smallest errors were obtained when model parameters were held constant at their 1 year mean values. The fact that higher temporal resolution input data improved model performance at MLO but not at the HaleNet sites indicates significant uncertainty in daily parameter values at the HaleNet sites. Errors arising from vertically interpolating between the MLO and Lāna'i sites and/or from horizontal variability are such that daily variations in clear sky radiation are not well represented.

[36] Because of Hawai'i's midoceanic location and distance from continental aerosol source areas, variability in atmospheric transmissivity is relatively low. This helps to explain why reasonably accurate model results were obtained when constant mean parameter values are used in place of daily interval data. In other regions, with higher day-to-day variability or a larger annual cycle in aerosol loading or humidity, the use of time-averaged input data is likely to have a greater impact on model performance.

[37] **Acknowledgments.** This work was partially supported by the Pacific Island Climate Change Cooperative. We thank Brett Holben and his staff for establishing and maintaining the two AERONET sites used in this investigation. We are grateful to Mike Nullet for his work in the maintenance of the HaleNet climate network, his rigorous screening of the solar radiation data obtained there, and help with the SPCTRAL2 code. The ozone values required for the model input were kindly provided by Robert Evans of the National Oceanic and Atmospheric Administration (NOAA). We are grateful to David Longnecker (NOAA) for providing a complete record of solar radiation data at Mauna Loa observatory. We also thank the staff of Haleakalā National Park and the Pacific Island Ecosystem Research Center (PIERC), USGS, for their long support of the HaleNet system. Special thanks goes to Lloyd Loope of PIERC.

## References

Alados, I., I. Foyo-Moreno, F. J. Olmo, and L. Alados-Arboledas (2002), Improved estimation of diffuse photosynthetically active radiation using two spectral models, *Agric. For. Meteorol.*, *111*, 1–12, doi:10.1016/S0168-1923(02)00010-2.

Alados-Arboledas, L., F. J. Olmo, I. Alados, and M. Perez (2000), Parametric models to estimate photosynthetically active radiation in Spain, *Agric. For. Meteorol.*, *101*, 187–201, doi:10.1016/S0168-1923(99)00163-X.

Anderson, G. P., J. H. Chetwynd, J. M. Theriault, P. Acharya, A. Berk, D. C. Robertson, F. X. Kneizys, M. L. Hoke, L. W. Abreu, and E. P. Shettle (1993), MODTRAN2: Suitability for remote sensing, *Atmos. Propag. Remote Sens. II*, *1968*, 514–525, doi:10.1117/12.154854.

Batlles, F. J., F. J. Olmo, J. Tovar, and L. Alados-Arboledas (2000), Comparison of cloudless sky parameterization of solar irradiance at various Spanish midlatitude locations, *Theor. Appl. Climatol.*, *66*, 81–93, doi:10.1007/s007040070034.

Bird, R. E. (1984), A simple solar spectral model for direct-normal and diffuse horizontal irradiance, *Sol. Energy*, *32*, 461–471, doi:10.1016/0038-092X(84)90260-3.

Bird, R. E., and C. Riordan (1986), Simple solar spectral model for direct and diffuse irradiance on horizontal and tilted planes at the Earth's surface for cloudless atmospheres, *J. Clim. Appl. Meteorol.*, *25*, 87–97, doi:10.1175/1520-0450(1986)025<0087:SSSMFD>2.0.CO;2.

Blackmore, W., and B. Taubvurtzel (1999), Environmental chamber tests of NWS radiosonde relative humidity sensors, paper presented at the International Conference on Interactive Information and Processing Systems, Am. Meteorol. Soc., Dallas, Tex., 10–15 Jan.

Brine, D. T., and M. Iqbal (1983), Diffuse and global solar spectral irradiance under cloudless skies, *Sol. Energy*, *30*, 447–453, doi:10.1016/0038-092X(83)90115-9.

Cao, G. G., T. W. Giambelluca, D. E. Stevens, and T. A. Schroeder (2007), Inversion variability in the Hawaiian trade wind regime, *J. Clim.*, *20*, 1145–1160, doi:10.1175/JCLI4033.1.

Clarke, A., and V. Kapustin (2010), Hemispheric aerosol vertical profiles: Anthropogenic impacts on optical depth and cloud nuclei, *Science*, *329*, 1488–1492, doi:10.1126/science.1188838.

Dubovik, O., B. N. Holben, T. F. Eck, A. Smirnov, Y. J. Kaufman, M. D. King, D. Tanré, and I. Slutsker (2002), Variability of absorption and optical properties of key aerosol types observed in worldwide locations, *J. Atmos. Sci.*, *59*, 590–608, doi:10.1175/1520-0469(2002)059<0590:VOAAOP>2.0.CO;2.

Eck, T. F., et al. (2005), Columnar aerosol optical properties at AERONET sites in central eastern Asia and aerosol transport to the tropical mid-Pacific, *J. Geophys. Res.*, *110*, D06202, doi:10.1029/2004JD005274.

Foyo-Moreno, I., J. Vida, F. J. Olmo, and L. Alados-Arboledas (2000), Estimating solar ultraviolet irradiance (290–385 nm) by means of the spectral parametric models: SPCTRAL2 and SMARTS2, *Ann. Geophys.*, *18*, 1382–1389, doi:10.1007/s00585-000-1382-2.

García, O. E., et al. (2008), Validation of AERONET estimates of atmospheric solar fluxes and aerosol radiative forcing by ground-based broadband measurements, *J. Geophys. Res.*, *113*, D21207, doi:10.1029/2008JD010211.

Gueymard, C. (1995), SMARTS2, Simple model of atmospheric radiative transfer of sunshine: Algorithms and performance assessment, *Tech. Rep. FSEC-PF-270-95*, 84 pp., Fla. Sol. Res. Cent., Cocoa.

Gueymard, C. (2001), Parameterized transmittance model for direct beam and circumsolar spectral irradiance, *Sol. Energy*, *71*, 325–346, doi:10.1016/S0038-092X(01)00054-8.

Gueymard, C. (2003a), Direct solar transmittance and irradiance predictions with broadband models. Part I: Detailed theoretical performance assessment, *Sol. Energy*, *74*, 355–379, doi:10.1016/S0038-092X(03)00195-6.

Gueymard, C. (2003b), Direct solar transmittance and irradiance predictions with broadband models. Part II: Validation with high quality measurements, *Sol. Energy*, *74*, 381–395, doi:10.1016/S0038-092X(03)00196-8.

Holben, B. N., et al. (1998), AERONET—A federated instrument network and data archive for aerosol characterization, *Remote Sens. Environ.*, *66*(1), 1–16, doi:10.1016/S0034-4257(98)00031-5.

Holben, B. N., et al. (2001), An emerging ground-based aerosol climatology: Aerosol optical depth from AERONET, *J. Geophys. Res.*, *106*(D11), 12,067–12,097, doi:10.1029/2001JD900014.

Ineichen, P. (2006), Comparison of eight clear sky broadband models against 16 independent data banks, *Sol. Energy*, *80*, 468–478, doi:10.1016/j.solener.2005.04.018.

Jacovides, C. P., D. G. Kaskaoutis, F. S. Tymvios, and D. N. Asimakopoulos (2004), Application of SPCTRAL2 parametric model in estimating spectral solar irradiances over polluted Athens atmosphere, *Renew. Energy*, *29*, 1109–1119, doi:10.1016/j.renene.2003.12.001.

Justus, C. G., and M. V. Paris (1985), A model of solar spectral irradiance and radiance at the bottom and top of cloudless atmosphere, *J. Clim. Appl. Meteorol.*, *24*(3), 193–205, doi:10.1175/1520-0450(1985)024<0193:AMFSSI>2.0.CO;2.

Kneizys, F. X., E. P. Shettle, L. W. Abreu, J. H. Chetwynd, G. P. Anderson, W. O. Gallery, J. E. A. Selby, and S. A. Clough (1980), *Users Guide to LOWTRAN 7*, 137 pp., Airforce Geophys. Lab., Hanscom AFB, Mass.

Larkin, E. D. (2002), Radiation balance over forested and agricultural sites in northern Thailand, M.S. thesis, Dept. of Geogr., Univ. of Hawai'i at Mānoa, Honolulu, Hawaii.

Leckner, B. (1978), The spectral distribution of solar radiation at the Earth's surface-elements of a model, *Sol. Energy*, *20*(2), 143–150, doi:10.1016/0038-092X(78)90187-1.

Long, C. N., and T. P. Ackerman (2000), Identification of clear skies from broadband pyranometer measurements and calculation of downwelling shortwave cloud effects, *J. Geophys. Res.*, *105*(D12), 15,609–15,626, doi:10.1029/2000JD900077.

Muller, C., and X. Kong (2009), Review of remotely sensed aerosol and cloud products and their applications, in *(A)ATSR Exploitation Plan*, *Tech. Rep. 6*, pp. 1–35, Univ. of Leicester, Leicester, U. K.

Myers, D. R., K. E. Emery, and C. Gueymard (2002), Terrestrial solar spectral modeling tools and applications for photovoltaic devices, *Conf. Rec. Twenty-Ninth IEEE Photovoltaic Spec. Conf.*, *2002*, 1683–1686, doi:10.1109/PVSC.2002.1190943.

Neckel, H., and D. Labs (1981), Improved data of solar spectral irradiance from 0.33 to 1.25 um, *Sol. Phys.*, *74*, 231–249, doi:10.1007/BF00151293.

Nullet, D., and P. Ekern (1988), Modeling clear day insolation at sea level in Hawaii, *Sol. Energy*, *40*(3), 187–189, doi:10.1016/0038-092X(88)90040-0.

Nullet, D., and T. W. Giambelluca (1992), Radiation climatology through the trade-wind inversion on the Lee slope of Haleakala, Maui, Hawaii, *Phys. Geogr.*, *13*, 66–80.

Olmo, F. J., J. Vida, I. Foyo-Moreno, J. Tovar, and L. Alados-Arboledas (2001), Performance reduction of solar irradiance parametric models due to limitations in required aerosol data: Case of the CPCR2 model, *Theor. Appl. Climatol.*, *69*, 253–263, doi:10.1007/s007040170030.

Porter, J. N., B. R. Lienert, S. K. Sharma, E. Lau, and K. Horton (2003), Vertical and horizontal aerosol scattering fields over Bellows Beach, Oahu, during the SEAS experiment, *J. Atmos. Oceanic Technol.*, *20*, 1375–1387, doi:10.1175/1520-0426(2003)020<1375:VAHASF>2.0.CO;2.

Reda, I., T. Stoffel, and D. Myers (2003), A method to calibrate a solar pyranometer for measuring reference diffuse irradiance, *Sol. Energy*, *74*(2), 103–112, doi:10.1016/S0038-092X(03)00124-5.

Riihimaki, L. D., and F. E. Vignola (2008), Establishing a consistent calibration record for Eppley PSPs, paper presented at the National Solar Energy Conference Solar 2008, Am. Sol. Energy Soc., San Diego, Calif., 3–8 May.

Smirnov, A., B. N. Holben, Y. J. Kaufman, O. Dubovik, T. F. Eck, I. Slutsker, C. Pietras, and R. N. Halthore (2002), Optical properties of atmospheric aerosol in maritime environments, *J. Atmos. Sci.*, *59*, 501–523, doi:10.1175/1520-0469(2002)059<0501:OPOAAI>2.0.CO;2.

Tadros, M., M. El-Metwally, and A. Hamed (2005), A comparative study on SPCTRAL2, SPCTR-1881 and SMARTS2 models using direct normal solar irradiance in different bands for Cairo and Aswan, Egypt, *J. Atmos. Sol. Terr. Phys.*, *67*, 1343–1356, doi:10.1016/j.jastp.2005.04.003.

Utrillas, M. P., J. V. Bosca, J. A. Martinex-Lozano, J. Canada, F. Tena, and J. M. Pinazo (1998), A comparative study of SPCTRAL2 and SMARTS2 parameterised models based on spectral irradiance measurements at Valencia, Spain, *Sol. Energy*, *63*(3), 161–171, doi:10.1016/S0038-092X(98)00058-9.

A. G. Frazier, T. W. Giambelluca, and R. J. Longman, Department of Geography, University of Hawai'i at Mānoa, 2424 Maile Way, Saunders Hall 445, Honolulu, HI 96822, USA. (rlongman@hawaii.edu)